LOCALIZATION AND MICRO-CHARACTERIZATION OF ORGANIC MATTER AND MINERAL PHASES IN BULK CHONDRITES BY MIR REFLECTANCE HYPERSPECTRAL IMAGING. Y. Arribard[1], D. Baklouti[1], A. Aléon-Toppani[1], F. Borondics[2], S. Della-Negra[3], Z. Djouadi[1] , B. Doisneau[4], C. Lantz[1], M. Noun[5], C. Sandt[2], R. Brunetto[1], [1]Universté Paris-Saclay, CNRS, Institut d'Astrophysique Spatiale, 91405, Orsay, France (yann.arribard@universite-paris-saclay.fr), [2]SOLEIL synchrotron, BP48, L'Orme des Merisiers Gif-sur-Yvette Cedex, France, 91192, [3]IJCLab, CNRS/IN2P3, Université Paris-Saclay, F-91406, Orsay, France, [4]IMPMC, MNHN, Sorbonne Univ., CNRS, Paris, France, [5]Lebanese Atomic Energy Commission, NCSR, Beirut 11-8281, Lebanon.

Introduction: Organic matter in chondrites carries information about formation and evolution processes of planetesimals in the early solar system. Chondritic organic matter is often analyzed after extraction from the meteorite matrix [e.g. 1,2]. In order to better understand the chemical history of this matter and its interaction with the phases surrounding it, it is necessary to analyze it *in situ*, i.e. directly in its mineral context. This avoid any physical and/or chemical extraction that could partially alter or modify it, and that inevitably loses information about the mineral phases. Previous research works started to explore this path [3,4,5,6].

In this study, we will focus on the Infrared (IR) reflectance analysis of sliced fragments of three chondrites: Paris (CM 2.8), Cold Bokkeveld (CM 2.2) and Tuxtuac (LL5). IR spectroscopy has the advantage of being able to characterize the organic and mineral content of a sample at the same time and without altering any of it. However, as showed in our previous work [6], the C-H stretching mode, generally signing the presence of organic matter, is very difficult to detect in the IR reflectance spectra of this kind of samples. In the present study, we improved the hyperspectral data processing to better characterize and map the mineral phases and to be able to map the C-H band location throughout relatively extended surface areas (> 500x500 µm²) with a spatial resolution of a few microns.

Material and methods: Meteorite samples were sliced with a diamond wire saw using a stainless-steel wire (0.13 mm diameter) set with 20 µm-size synthetic diamonds (MNHN, Paris), without involving any liquid during the cut to prevent any modification of the hydration characteristics and organic content of the samples.

Mid-IR (4000-800 cm^{-1}, 2.5-12.5 µm) hyperspectral imaging was carried out in reflectance mode with an Agilent Cary 670 IR microscope (x15 objective) equipped with a Focal Plane array detector and a Globar source (SMIS beamline, SOLEIL synchrotron, Gif-sur-Yvette) [6,7]. The surfaces explored by this technique were squares of 704x704 µm² area with a pixel size of 5.5x5.5 µm². The spatial resolution is diffraction-limited at all wavelengths. The spectral resolution was 4 cm^{-1}. Compared to our previous work [6], IR data processing was greatly improved by using a k-means clustering method applied with the open source software Quasar [8].

In addition, complementary measurements are performed with Raman micro-spectroscopy on selected spots in order to support the identification of the mineral phases and to characterize the carbonaceous polyaromatic content of the different chondrite samples. Raman analyses were conducted with a DRX Raman spectrometer from Thermo Fischer using a 532 nm laser with a power of 0.5 mW. A x50 objective with a 25 µm slit aperture was used, leading to a spot on the sample smaller than 2 µm (SMIS beamline, SOLEIL synchrotron, Gif-sur-Yvette) [6].

Results: In a first step, an optimized k-means clustering process applied to the 5.9-11.8 µm spectral range resulted in clusters' average spectra (Fig. 1e) corresponding each to a main mineral category or group that can be mapped as showed in Fig. 1c. Mineral identifications were determined according to measurements of standards we made with the same setup, literature data [e.g. 9, 10, 6 and references there in], and Raman measurements for validation. Furthermore, this clustering method allows to estimate the proportions of the main mineral components composing the analyzed surface. For example, for the area of Cold Bokkeveld mapped in Figure 1, we found a composition of: 81% of phyllosilicates, 7% of olivines, 10% of pyroxenes, and 2% of carbonates and sulfates. These values are quite representative of the whole chondrite composition according to literature [11].

In a second step, a sub-clustering was applied to each primary cluster to study separately and map the structural and/or mineralogical variability inside each main mineral group. As an example, we present in Fig. 1d, a color map showing the position variation of the Si-O stretching band maximum in the spectra corresponding to the phyllosilicate cluster extracted from Cold Bokkeveld sample measurements. In this case, this variation is either an indication of the presence of some contribution from another component to the spectrum (olivine often, here) or, when confirmed by other parameters' maps, an indication of some structural and mineralogical differences in the phyllosilicate component.

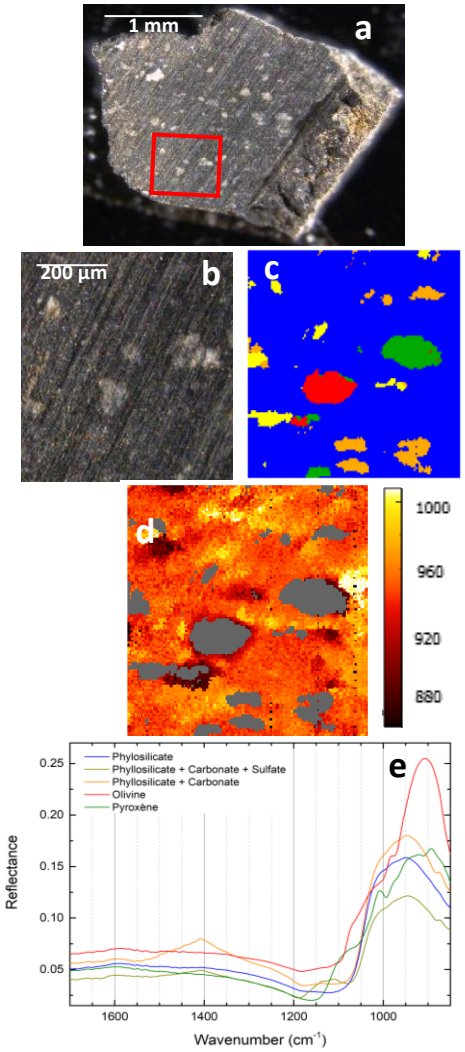

Figure 1 : (a), a visible image of the slice of Cold Bokkeveld (the red square indicates the surface analyzed below). **(b)**, a visible image of the 704x704 µm² area analyzed by IR hyperspectral imaging. **(c),** localization of the main mineral components obtained with k-means clustering analysis: phyllosilicates (blue), olivines (red), pyroxenes (green), phyllosilicates mixed to carbonates (orange), phyllosilicates mixed to carbonates and sulfates (yellow). **(d),** mapping of the maximum Si-O stretching band position (in cm^{-1}) of the cluster of phyllosilicates. **(e)**, Clusters' average spectra on to the 5.9-11.8 µm spectral range

In a third step, in order to study the mineral phases' hydration state, a similar k-means clustering procedure was applied to the 2.6-3.7 µm spectral range, in order to separate the phases according to their spectral signature in the O-H stretching region. Then, to reveal the hydration state variation in each concerned mineral phase, a sub-clustering was applied.

In a fourth step and for each of the three meteorite samples, a dedicated sub-clustering of each mineral cluster applied to the 3.2-3.7 µm spectral range allowed to detect the pixels showing a clear C-H signature, and thus, to map the location of organic matter throughout the sample surface analyzed.

Finally, our first results indicate that organic matter seems to be mainly co-located with the hydrated silicate components, as observed by the previous studies [4,5,6].

Conclusion and prospect: MIR reflectance hyperspectral imaging associated with a data processing based on k-means clustering allowed us to study and map at a few µm resolution, the mineral phases composing millimeter-sized surfaces of chondrites, their hydration state, and their co-location with the detected organic matter.

Thus, this non-destructive technique associated with the improved data process, presents promising prospects for the analysis of valued samples larger than ~100 µm such as, part of the Ryugu samples collected and recently returned by the Hayabusa2 mission or some of the samples the OSIRIS-REx space probe will return to Earth in 2023.

Acknowledgments: We thank B. Zanda and the Museum National d' Histoire Naturelle (MNHN, Paris) for providing us with the Paris meteorite sample. The Cold Bokkveld meteorite samples was provided by the Vatican Observatory. We thank L. Bonal for providing us with the Tuxtuac meteorite samples. The micro-spectroscopy measurements were supported by grants from Region Ile-de-France (DIM-ACAV) and SOLEIL. This work has been funded by the Centre National d'Etudes Spatiales (CNES-France) and by the ANR project CLASSY (Grant ANR-17-CE31-0004-02) of the French Agence Nationale de la Recherche.

References: [1] Pizzarello et al. (2006) *Meteorites and the early solar System II*, 625-651 [2] Alexander et al. (2017), *Chemi der Erde-Geochemistry*, *77*,227-256. [3] Garvie et al. (2007), *Meteor. Planet Sci., 42*, 2111-2117. [4] Le Guillou et al. (2014), *Geochimica et cosmochimica*, *131*, 344-367. [5] Le Guillou et al. (2014), *Geochimica et cosmochimica*, *131*, 368-392. [6] Noun et al. (2019), *Life*, *9*, 44. [7] Brunetto et al. (2018) *Planetary and Space Sci*., *158*, 38-45. [8] Toplak et al. (2020) *Zenodo*. [9] Salisbury et al. (1993), *Remote geochemical analysis*: *Chapter 4*. [10] Beck et al. (2014) *Icarus*, *229*, 263-277. [11] Howard et al. (2009), *Geochimica et cosmochimica*, *73*, 4576-4589.